Title	Optimal control for semi-active suspension with inerter
Author(s)	Hu, Y; Li, C; Chen, MZ
Citation	The 31st Chinese Control Conference (CCC 2012), Hefei, China, 25-27 July 2012. In Chinese Control Conference, 2012, p. 2301-2306
Issued Date	2012
URL	http://hdl.handle.net/10722/160294
Rights	Chinese Control Conference. Copyright © Institute of Electrical and Electronics Engineers.

Proceedings of the 31st Chinese Control Conference
July 25-27, 2012, Hefei, China

Optimal control for semi-active suspension with inerter

Yinlong Hu[1], Chanying Li[2], and Michael Z. Q. Chen[1,3,*]

1. School of Automation, Nanjing University of Science and Technology, Nanjing, China.

2. Academy of Mathematics and Systems Sciences, Chinese Academy of Science, Beijing, China.

3. Department of Mechanical Engineering, The University of Hong Kong, Hong Kong. Email: mzqchen@hku.hk.

Abstract: The benefits of the inerter in passive suspension have been well demonstrated. To investigate suspension performances with the inerter in semi-active suspension, eight well studied passive suspension configurations with a parallel connection to a variable shock absorber are analyzed in this paper. By applying the optimal control theory, an optimal solution for each configuration is obtained and numerically solved by the forward/backward sweep method. The result shows that under the considered performance measure, the use of inerter can improve ride comfort in general, where the effect can even be significant for some specific configurations, but has no obvious advantage in road holding and suspension travel performance compared with the conventional semi-active suspension.

Key Words: Inerter, semi-active suspension, optimal control.

1 Introduction

Semi-active suspensions have attracted much attention because of the low energy consumption when compared with the active ones and their high performances when compared with the passive ones. The conventional semi-active suspension configuration, that is, a spring in parallel with a variable shock absorber, has been investigated by many researchers and a large number of meaningful results have been obtained [1–4].

Inerter is a recently proposed concept and device with the property that the applied force at the two terminals is proportional to the relative acceleration between them [5, 6]. The inerter expands the class of mechanical realizations of complex impedances compared with the ones using only springs and dampers and has been applied to various mechanical systems, including vehicle suspensions [7, 8], motorcycle steering systems [9] and building vibration control [10]. It has also rekindled interest in passive network synthesis [11–14].

To investigate the benefits of using inerter in semi-active suspensions and what performance level the semi-active suspension involving inerter will be achieved, eight well studied passive suspension configurations [7, 8] with a parallel connection with a semi-active damper are analyzed in this paper. By applying the optimal control theory, an optimal solution of each configuration is obtained and numerically solved by the forward/backward sweep method [20]. Two kinds of road excitations [15, 22], the randomly profiled road and single bump road, are employed to test the performance of each configuration using a well defined performance measure, which combines ride comfort, road holding and suspension travel. After being compared with the conventional semi-active suspension configuration, the effects of semi-active suspension with inerter are highlighted.

The organization of this paper is as follows. In Section 2, the optimal control problem is formulated under a quarter car model with the considered semi-active suspension configurations. The algorithm to solve such a problem is also included in this section. Section 3 presents two simulation results with two kinds of road excitations. Some general remarks for semi-active suspension with inerter are also given in this section. Conclusions are drawn in Section 4.

* Corresponding author.

2 Vehicle model and optimal control problem formulation

2.1 Quarter-car model

Consider the quarter-car model in Fig. 1. As an elementary model to study suspension systems, the quarter-car model consists of the sprung mass m_s, the unsprung mass m_u and the tyre vertical stiffness k_t [8, 15, 18, 19]. The suspension strut provides an equal and opposite force on the sprung mass and unsprung mass. In this study, the suspension system consists of two parts, the passive part and the semi-active part. The passive part is one of the conventional passive suspension configurations shown in Fig. 2, which have been widely investigated in passive suspension design [7, 8]. The admittance for each configuration is $Y_i(s) = \frac{k_s}{s} + Q_i(s)$, $i = 1, \ldots, 8$ and $Q_i(s)$ is shown in Table 1. The semi-active part is involved a variable shock absorber such as Electrohydraulic Dampers (EH Dampers), Magnetorheological Dampers (MR Dampers) and Electrorheological Dampers (ER Dampers) [16]. Here, $F_d = c_v(\dot{z}_s - \dot{z}_u)$ with $c_v \in [c_{\min},\ c_{\max}]$.

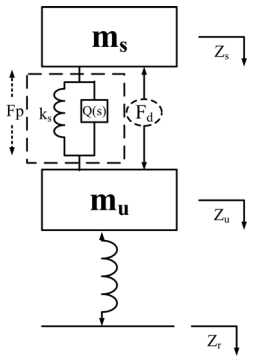

Fig. 1: Semi-active quarter-car model.

Define $F = Q(s)(\dot{z}_s - \dot{z}_u)$. The the dynamic equations are as follows

$$\begin{aligned} m_s\ddot{z}_s &= -k_s(z_s - z_u) - F - F_d, \\ m_u\ddot{z}_u &= k_s(z_s - z_u) + F + F_d - k_t(z_u - z_r). \end{aligned}$$

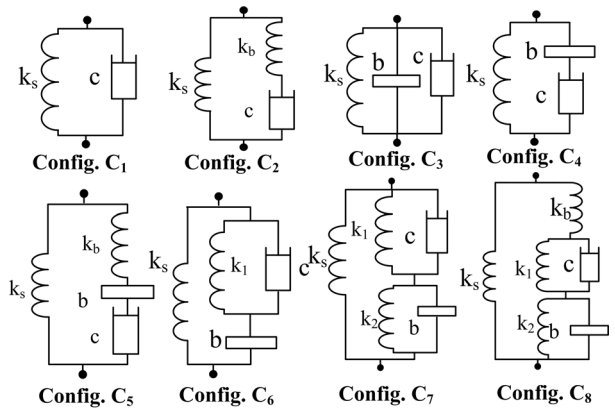

Fig. 2: The configurations in the passive part of the suspension.

The state space representation is then obtained

$$\dot{x} = \bar{A}x + B_2F + B_2F_d + B_1\omega, \tag{1}$$

where $x = \begin{bmatrix} z_s - z_u & \dot{z}_s & z_u - z_r & \dot{z}_u \end{bmatrix}^T$, $\omega = \dot{z}_r$,

$$\begin{aligned} \bar{A} &= \begin{bmatrix} 0 & 1 & 0 & -1 \\ -\frac{k_s}{m_s} & 0 & 0 & 0 \\ 0 & 0 & 0 & 1 \\ \frac{k_s}{m_s} & 0 & -\frac{k_t}{m_u} & 0 \end{bmatrix}, \\ B_1 &= \begin{bmatrix} 0 & 0 & -1 & 0 \end{bmatrix}^T, \\ B_2 &= \begin{bmatrix} 0 & -\frac{1}{m_s} & 0 & \frac{1}{m_u} \end{bmatrix}^T, \end{aligned}$$

Next, we will show that the state space representation (1) for each configuration can be transformed into a uniform bilinear state equations.

For C_1 and C_3, it is straightforward to obtain the representation below

$$\dot{x} = A_ix + D_ixc_v + B\omega, \tag{2}$$

where

$$A_1 = \begin{bmatrix} 0 & 1 & 0 & -1 \\ -\frac{k_s}{m_s} & -\frac{c}{m_s} & 0 & \frac{c}{m_s} \\ 0 & 0 & 0 & 1 \\ \frac{k_s}{m_u} & \frac{c}{m_u} & -\frac{k_t}{m_u} & -\frac{c}{m_u} \end{bmatrix},$$

$$A_3 = \begin{bmatrix} 0 & 1 & 0 & -1 \\ -m_uk_sd & -m_ucd & -k_tbd & m_ucd \\ 0 & 0 & 0 & -1 \\ m_sk_sd & m_scd & -(m_s+b)k_td & -m_scd \end{bmatrix},$$

Table 1: $Q(s)$ for each configuration in Fig. 2, where s denotes the Laplace variable.

$Q_1(s) = c$	$Q_2(s) = \frac{1}{\frac{s}{k_b}+\frac{1}{c}}$
$Q_3(s) = bs + c$	$Q_4(s) = \frac{1}{\frac{1}{c}+\frac{1}{bs}}$
$Q_5(s) = \frac{1}{\frac{s}{k_b}+\frac{1}{bs}+\frac{1}{c}}$	$Q_6(s) = \frac{1}{\frac{1}{\frac{1}{s}+c}+\frac{1}{bs}}$
$Q_7(s) = \frac{1}{\frac{1}{\frac{1}{s}+c}+\frac{1}{\frac{k_2}{s}+bs}}$	$Q_8(s) = \frac{1}{\frac{s}{k_b}+\frac{1}{\frac{1}{s}+c}+\frac{1}{\frac{k_2}{s}+bs}}$

where $d = \frac{1}{m_sm_u+(m_s+m_u)b}$.

Define $l = \begin{bmatrix} 0 & 1 & 0 & -1 \end{bmatrix}$, then $D_1 = D_3 = B_2l$, $B = B_1$. Furthermore, A_1, D_1 and A_3, D_3 correspond to C_1 and C_3, respectively.

For C_2 and C_4–C_8, assuming

$$Q(s) = \frac{b_{n-1}s^{n-1} + \ldots + b_1s + b_0}{s^n + a_{n-1}s^{n-1} + \ldots + a_1s + a_0} + d_p,$$

a corresponding control canonical form is realized

$$\begin{aligned} \dot{x}_p &= A_px_p + B_pu_p, & (3) \\ y &= C_px_p + d_pu_p, & (4) \end{aligned}$$

where $u_p = \dot{z}_s - \dot{z}_u$, $y = F$ and

$$A_p = \begin{bmatrix} 0 & 1 & 0 & \ldots & 0 \\ 0 & 0 & 1 & \ldots & 0 \\ \vdots & \vdots & \vdots & \vdots & \vdots \\ 0 & 0 & 0 & \ldots & 1 \\ -a_0 & -a_1 & -a_2 & \ldots & -a_{n-1} \end{bmatrix},$$

$$B_p = \begin{bmatrix} 0 & 0 & \ldots & 0 & 1 \end{bmatrix}^T,$$

$$C_p = \begin{bmatrix} b_0 & b_1 & b_2 & \ldots & b_{n-1} \end{bmatrix}.$$

By (1), (3) and (4), we obtain

$$\dot{y} = Ay + Dyc_v + B\omega, \tag{5}$$

where $y = \begin{bmatrix} x & x_p \end{bmatrix}^T$ and

$$A = \begin{bmatrix} \bar{A} + B_2d_pl & B_2C_p \\ B_pl & A_p \end{bmatrix},$$

$$D = B_2l, \quad B = \begin{bmatrix} B_1 & 0 \end{bmatrix}^T,$$

where A, D, and B are of compatible dimensions.

Observing (2) and (5), it is obvious that the state space equations for the considered configurations have a uniform representation. Hence, in the following sections, (5) will be used as a representation for all the eight configurations. It should be noted that a similar representation for C_1 appeared in [15, 19], but they all treat the variable damping ratio and the state together and obtained a piecewise equation relating to the states. In this study, we give a slightly different formulation, which rely on the damping ratio directly. Then the optimal control theory can be employed as a method to observe how the damping ratio changes with different road profiles.

2.2 Performance measure

It is well known that suspension system design is a compromise among a number of performance requirements such as passenger comfort, handling, road holding and limits of suspension travel. The objective of our problem is to control the variable damping ratio to minimize the performance defined in [15, 17, 19, 22]

$$J = \int \left(\ddot{z}_s^2 + \rho_1(z_s - z_u)^2 + \rho_2(z_u - z_r)^2\right) d_t, \tag{6}$$

where ρ_1 and ρ_2 are weight coefficients determined by designer. Performance measure (6) is a combination of the RMS value of sprung mass accelerations, suspension travels and tire deflections, which indicate ride comfort, suspension travel and road holding, respectively. In this present work, we set $\rho_1 = 10^3$ and $\rho_2 = 10^4$, the same as in [15, 22].

2.3 Optimal control formulation

Since we intend to obtain the best performance and benefits for semi-active suspension with inerter, some assumptions are made, similar to [18]:

1) The road disturbance information is fully obtained in advance for the whole time interval $[t_0,\ t_f]$.
2) There is no measurement noise and the state variables $(y(t))$ are measured perfectly,
3) System uncertainty is not considered, that is, the model is an accurate model of the real system.
4) The semi-active damper is ideal without actuating delay (infinite bandwidth) or force saturation.

Theorem 1. *The objective index (6) can be written as*

$$J = \int_{t_0}^{t_f} (y^T P_2 y c_v^2 + y^T P_1 y c_v + y^T P_0 y) d_t, \qquad (7)$$

where

$$P_2 = d(2)^T d(2), P_1 = a(2)^T d(2) + d(2)^T a(2),$$

$$P_0 = a(2)^T a(2) + \rho_1 l_1^T l_1 + \rho_2 l_2^T l_2,$$

$$l_1 = \begin{bmatrix} 1 & 0 & 0 & \dots & 0 \end{bmatrix}, l_2 = \begin{bmatrix} 0 & 0 & 1 & 0 & \dots & 0 \end{bmatrix}.$$

$a(2)$ and $d(2)$ are the second row of A and D, respectively.

Define the Hamiltonian

$$H = y^T P_2 y c_v^2 + y^T P_1 y c_v + y^T P_0 y + \lambda^T (Ay + Dyc_v + B\omega) \qquad (8)$$

and the adjoint function

$$\dot{\lambda} = -\frac{\partial H}{\partial y} = -\left((Q^T + Q)y + A^T\lambda + D^T\lambda u\right), \qquad (9)$$

where $Q = P_2 c_v^2 + P_1 c_v + P_0$. The boundary condition and transversality condition is

$$y(t_0) = y_0,\ \ \lambda(t_f) = 0. \qquad (10)$$

Denote

$$c_{v0} = -(2y^{*T} P_2 y^*)^{-1}(y^{*T} P_1 y^* + \lambda^{*T} D y^*),$$

where y^* and λ^* are the solutions of (5), (9) and (10).

Then the optimal c_v^* to minimize (7) is

$$c_v^* = \begin{cases} c_{\max}, & c_{v0} \geq c_{\max} \\ c_{\min}, & c_{v0} \leq c_{\min} \\ c_{v0}, & \textit{otherwise.} \end{cases} \qquad (11)$$

Proof. By the Minimum Principle of Pontryagin, to minimize (7), it suffices to minimize H with respect to c_v. Considering (5), (9) and (10), we have

$$\frac{\partial H}{\partial c_v} = 2y^T P_2 y c_v + y^T P_1 y + \lambda^T D y = 0,$$

$$c_{v0} = -(2y^{*T} P_2 y^*)^{-1}(y^{*T} P_1 y^* + \lambda^{*T} D y^*).$$

y^* and λ^* denote the solutions of (5), (9) and (10). Since $\frac{\partial^2 H}{\partial c_v^2} = 2y^T P_2 y = E(y_2 - y_4)^2 > 0$, E is a real positive constant value equal to $2d^2 {m^2}_u$ for C_3 and $\frac{2}{m_s^2}$ for the others, c_{v0} is the optimal solution. Considering the damping ratio constraints, we obtain (11). ■

Note that there is a singular point in (11), $2y^T P_2 y = E(y_2 - y_4)^2 = 0$, that is $\dot{z}_s - \dot{z}_u = 0$. Practically, it means that the relative velocity of the sprung mass and unsprung mass is zero, where it is reasonable to set the damping ratio equal to the previous one [15].

The problem formulated using (7)–(11) defines a two-point boundary value problem, which can be numerically solved by the forward/backward sweep method [20].

***Algorithm statement*:**

Step 1 Make an initial guess for c_v over the interval.

Step 2 Using the initial condition $y(t_0) = y_0$ and the guess c_v, solve y forward in time according to its differential equation in the optimality system.

Step 3 Using the transversality condition $\lambda(t_f) = 0$ and the previous c_v and y, solve λ backward in time according to its differential equation in the optimality system.

Step 4 Update the control by entering the new y and λ values into the characterization of c_v.

Step 5 Check convergence. If values of the variables in this iteration and the last iteration are negligibly small, output the current values as solutions. If not, return to Step 2.

3 Numerical results

The parameters in [21] for the quarter-car model is employed as shown in Table 2.

Table 2: Model parameters.

Parameter	Value
Sprung mass	400 kg
Unsprung mass	50 kg
Static stiffness, K	20 kN/m
The minimum damping ratio for c_v	300 Ns/m
The maximum damping ratio for c_v	4000 Ns/m
Damping ratio c in passive part	1500 Ns/m
Relaxation spring stiffness, k_b	$2K$
Centering spring stiffness, k_1	$0.4K$
Centering spring stiffness, k_2	$0.2K$
Primary spring stiffness, k_s	$0.86667K$ for C_6 $0.875K$ for C_7

To see the performance level of the eight configurations, the suspension performance was evaluated under two types of road inputs: randomly profiled road and a single bump. The two road profiles have been well defined in [15, 22] described as follows.

The randomly profiled road is a stationary stochastic process with spectral density

$$S_\omega(\omega) = \frac{\sigma^2}{\pi} \times \frac{\alpha v}{\omega^2 + (\alpha v)^2}, \qquad (12)$$

where v is vehicle forward velocity, ω is circular frequency and α, σ are constant parameters dependent on the type of road surface. The process $\omega(t)$ in (12) can be generated by passing a white noise process through the filter

$$\dot{\omega} + \alpha v \omega = \xi,$$

where ξ is a Gaussian white noise process with intensity $2\sigma\alpha v$. In this example, $\alpha = 0.15$ cm^{-1} and $\sigma^2 =$

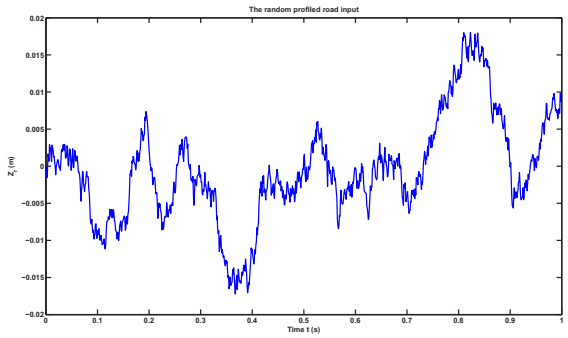

Fig. 3: A group of randomly profiled road input.

9×10^{-6} m^2, the same as in [15, 22], the forward velocity is 25 m/s. The input signal is shown in Fig. 3.

The single bump road signal is generated by

$$\omega(t) = \begin{cases} c(1 - \cos 20\pi(t - 0.3)), & t \in [0.3\ 0.4], \\ 0, & \text{otherwise.} \end{cases} \quad (13)$$

where $2c$ is the bump height in [m] and t time in [sec], assuming $2c = 0.1$ m. The input signal is shown in Fig. 4.

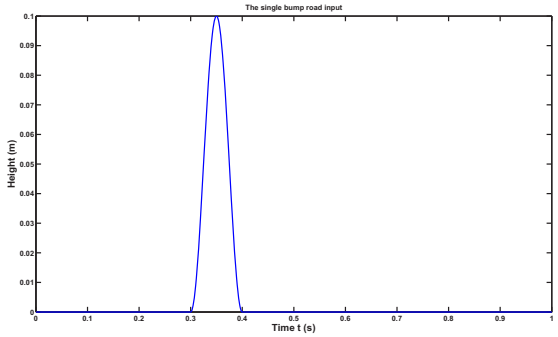

Fig. 4: The single bump road input.

The randomly profiled road is used to test the vehicle behaviors when traveling on the normal road. Similar to (6), a series of performance measures are defined in (14) to (16) to simulate the ride comfort, road holding and suspension travel performance, respectively.

$$J_{com} = \int_{t_0}^{t_f} (\ddot{z}_s)^2 d_t, \quad (14)$$

$$J_{rhd} = \int_{t_0}^{t_f} (z_s - z_u)^2 d_t, \quad (15)$$

$$J_{str} = \int_{t_0}^{t_f} (z_u - z_r)^2 d_t. \quad (16)$$

In order to investigate the effects of employing the inerter, we set b, the inertance, ranging from 50 kg to 500 kg. After simulating 10 different road inputs for each inertance, the average performance measure of C_1 was used as a benchmark and the relative performance results of the other configurations are obtained shown in Fig. 5 to Fig. 7. The percentages of improvement or decrease for each configuration versus C_1 are shown in Table 3, where '+' denotes improvement and '−' denotes deterioration.

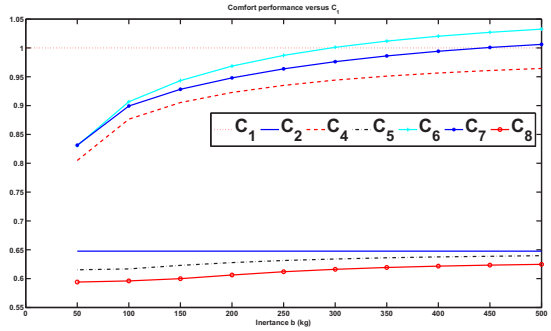

Fig. 5: The ride comfort performance with randomly profiled road. The one for C_3 is so large that it is not shown in this figure, the specific data of which is in Table 3.

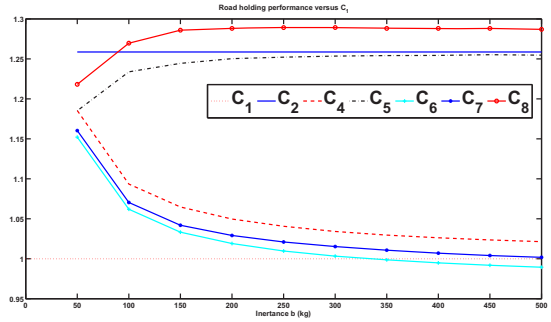

Fig. 6: The road holding performance with randomly profiled road. The one for C_3 is so large that it is not shown in this figure, the specific data of which is in Table 3.

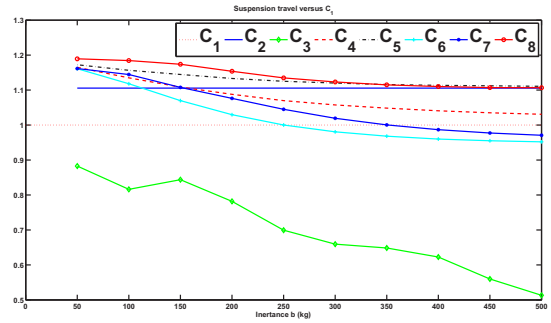

Fig. 7: The suspension travel with randomly profiled road.

As shown in Table 3, the use of inerter for C_3 has no advantage compared with C_1, though it can reduce the suspension travel space greatly, since for a normal inertance (100–350 kg) the ride comfort and road holding performance of C_3 are 50.80% to 839.06% worse than C_1. For this reason, C_3 was deleted from Fig. 5 and Fig. 6.

Observing Fig. 5, it is obvious that all the configurations provide a better comfort performance than C_1 (except C_6 with a large inertance), especially for C_8, 39.37% improvement was obtained with $b = 200$ kg as Table 3 shows. It is interesting to point out that two groups were classified with the increasing of inertance shown in Fig. 5 to Fig. 7, although it is not obvious in Fig. 7. The first group consists of C_4, C_6 and C_7, the three of which tend to coincide with C_1; while the other consists of C_5 and C_8 with a relaxation spring k_b,

which tend to coincide with C_2. It is understandable since, with the increase of inertance, the branch with the inerter will tend to 'shorten' or 'stiffen' the connection between sprung mass (or unsprung mass) and dampers, which will reduce the configurations of each group to C_1 or C_2, respectively. As for C_6, C_7 and C_8, when the inertance is large enough, the static stiffness of the suspension strut is no longer K but k_s+k_1 for C_6 and C_7, $k_s+(k_b^{-1}+k_1^{-1})^{-1}$ for C_8, the increase of static stiffness will explain why the ride comfort performance of C_6 is larger than C_1 as shown in Fig. 5 and Table 3. This is consistent with the passive suspension design in [7, 8] that the optimal ride comfort measure increases monotonically with static stiffness. Besides, by comparing C_1 and C_2, C_4 and C_5, C_7 and C_8, it is obvious that the use of relaxation spring k_b provides a better ride comfort in the considered suspension combination, which is different from the passive suspension design where relaxation spring is not intended to improve ride comfort [7, 8].

For the road holding and suspension travel performance, similar results have been obtained to the ride comfort performance. The formation of two groups can be explained the same as above. It is notable that inerter brings no improvement compared with C_1 as shown in Fig. 6 and Fig. 7, and also in Table 3. By comparing C_1 and C_2, C_4 and C_5, C_7 and C_8 in pair in Fig. 6, Fig. 7 and Table 3 again, we find that the relaxation spring k_b does not bring any advantage in road holding and has very slight influence on suspension travel.

Considering ride comfort, road holding and suspension travel together and comparing them with each other in Table 3, we find that C_5 and C_8 can improve ride comfort greatly at the expense of damaging road holding and suspension travel greatly as well. For example, when the inertance is 200 kg, the percentages of improvement of ride comfort for C_5 and C_8 are 37.22% and 39.37% respectively, but the percentages of road holding decrease are 25.03% and 28.82%, the decrease of suspension travel are 13.32% and 15.37%, respectively. As for C_4, C_6 and C_7, they can improve ride comfort slightly, but also decrease road holding slightly. The shortcoming is the highly increase of suspension travel space. Take $b = 200$ kg for example again, the percentages for ride comfort improvement are 7.72%, 3.15% and 5.20% for C_4, C_6 and C_7, respectively. In the meanwhile, the numbers of decrease for road holding and suspension travel are 4.97%, 1.90%, 2.91% for road holding and 8.78%, 2.97%, 7.62% for suspension travel. In conclusion, since suspension system design is a tradeoff among a number of performance requirements, the considered suspension structure and seven configurations indeed enrich the choice of suspension design.

The bump test is intended to simulate the performance for vehicle traveling on a bump like road. The inertance of this simulation is 200 kg. The results confirm the discussion above. As shown in Fig. 8, C_2, C_5 and C_8 can improve ride comfort greatly, but also reduce road holding performance heavily and demand more suspension travel space compared with C_1. Besides, from Fig. 9 we see that the displacement of sprung mass for C_5 and C_8 are less than the other configurations, which means that the vehicle body will be less affected by the road excitation, and hence ride comfort will be greatly improved. Fig. 9 also shows that the other configurations except C_3 provide a slight improvement in ride comfort compared with C_1. The displacement of unsprung mass represents the capability of tracing the road input. Observing Fig. 10, the overshoots for C_2, C_5 and C_8 are more than C_1, C_4, C_6, C_7 and C_2. The unsprung mass displacements of C_5 and C_8 are more oscillatory as well, which consistent with the randomly profiled road test that C_2, C_5 and C_8 will decrease road holding badly. For C_4, C_6 and C_7, it seems no difference from C_1.

Table 3: The specific data for ride comfort (COM), road holding (RHD) and suspension travel (STR), where '+' denotes improvement compared with C_1 and '−' denotes deterioration compared with C_1.

Inertance		b=100 kg	b=150 kg	b=200 kg	b=250 kg	b=300 kg	b=350 kg
C_1	COM	100%	100%	100%	100%	100%	100%
	RHD	100%	100%	100%	100%	100%	100%
	STR	100%	100%	100%	100%	100%	100%
C_2	COM	+35.23%	+35.23%	+35.23%	+35.23%	+35.23%	+35.23%
	RHD	-25.87%	-25.87%	-25.87%	-25.87%	-25.87%	-25.87%
	STR	-10.57%	-10.57%	-10.57%	-10.57%	-10.57%	-10.57%
C_3	COM	-166.34%	-267.62%	-384.15%	-516.55%	-671.92%	-839.06%
	RHD	-50.80%	-82.21%	-122.24%	-168.96%	-223.45%	-281.67%
	STR	+18.39%	+15.63%	+21.82%	+30.07%	+34.06%	+35.15%
C_4	COM	+12.36%	+9.48%	+7.72%	+6.49%	+5.58%	+4.90%
	RHD	-9.35%	-6.48%	-4.97%	-4.06%	-3.41%	-2.95%
	STR	-13.50%	-10.87%	-8.78%	-6.98%	-5.75%	-4.84%
C_5	COM	+38.31%	+37.70%	+37.22%	+36.86%	+36.60%	+36.39%
	RHD	-23.38%	-24.45%	-25.03%	-25.22%	-25.35%	-25.42%
	STR	-15.66%	-14.47%	-13.32%	-12.52%	-12.02%	-11.57%
C_6	COM	+9.34%	+5.67%	+3.15%	+1.30%	-0.10%	-1.18%
	RHD	-6.20%	-3.32%	-1.90%	-0.97%	-0.32%	+0.14%
	STR	-11.81%	-6.98%	-2.97%	-0.01%	+1.93%	+3.18%
C_7	COM	+10.07%	+7.17%	+5.20%	+3.63%	+2.39%	+1.39%
	RHD	-7.04%	-4.19%	-2.91%	-2.10%	-1.52%	-1.07%
	STR	-14.45%	-10.77%	-7.62%	-4.51%	-1.94%	-0.05%
C_8	COM	+40.40%	+40.01%	+39.37%	+38.81%	+38.39%	+38.06%
	RHD	-26.96%	-28.60%	-28.82%	-28.92%	-28.93%	-28.82%
	STR	-18.45%	-17.39%	-15.37%	-13.49%	-12.32%	-11.49%

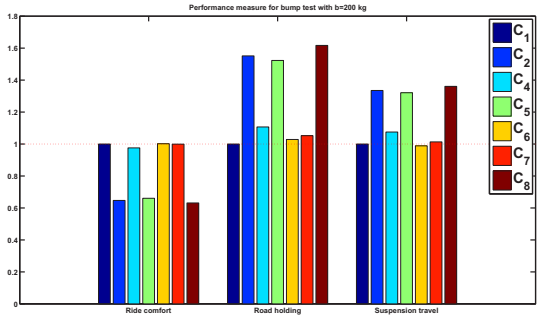

Fig. 8: The performance for bump profiled road.

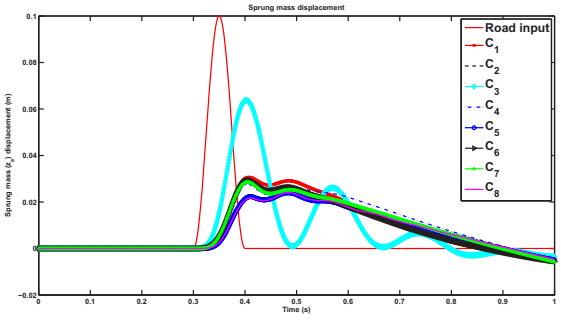

Fig. 9: The sprung mass displacement.

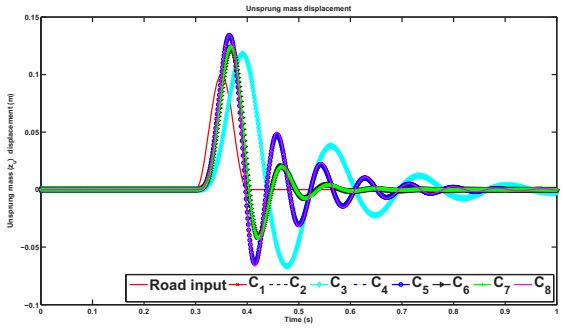

Fig. 10: The unsprung mass displacement.

4 Conclusions

A theoretical research on semi-active suspension design with inerter was carried out. To investigate the benefits of semi-active suspension employing inerter, the suspension strut was divided into two parts. Eight configurations, some of which employ inerter, constitute the passive part and the semi-active part was a variable shock absorber. Optimal control theory was applied to obtain the optimal bound for such a construction with inerter with respect to ride comfort, road holding and suspension travel performance for a quarter car model. After using the forward/backward sweep method to solve the two-point boundary problem numerically, some simulation results were obtained with two different kinds of road profile excitations. The results showed that inerter can provide better ride comfort than the conventional layout of semi-active suspension C_1, especially for C_2, C_5 and C_8 which have a relaxation spring, 35% to 40% improvement will be obtained compared to the conventional one C_1. The tradeoff for using the inerter is the decrease of road holding and suspension travel performance compared with C_1. For the other seven configurations compared with C_1, C_4, C_6 and C_7 can improve ride comfort slightly but reduce road holding slightly as well. In comparison, C_2, C_5 and C_8 can improve ride comfort heavily but also reduce road holding heavily. C_3 has no improvement in either ride comfort or road holding. In conclusion, for various performance requirements in suspension design, the considered configurations with inerter indeed enrich the choices for semi-active suspension design.

Acknowledgment

This work is supported in part by NNSFC 61004093, HKU CRCG 201008159001, and "973 Project" 2012CB720200.

References

[1] J. Emura, S. Kakizaki, F. Yamaoka, and M. Nakamura, Development on the semi-active suspension system based on the sky-hook damper theory, *Society of Automotive Engineers*, pp. 17–26, 1994.

[2] J.H. Koo, M. Ahmadian, M. Setareh, and T. Murray, In search of suitable control methods for semi-active tuned vibration absorbers, *Journal of Vibration and Control*, 10:163–174, 2004.

[3] D. Karnopp, Active damping in road vehicle suspension systems, Veh. Syst. Dyn., 12:296–316, 1983.

[4] M. Canale, M. Milanese, and C. Novara. Semi-active suspension control using fast model-predictive techniques, *IEEE Transaction on Control System Technology*, 14:1034–1046, 2006.

[5] M.C. Smith, Synthesis of mechanical networks: the inerter, *IEEE Trans. on Automatic Control*, vol. 47, no. 10, 1648–1662, 2002.

[6] M.Z.Q. Chen, C. Papageorgiou, F. Scheibe, F-C. Wang, and M.C. Smith, The missing mechanical circuit element, *IEEE Circuits Syst. Mag.*, vol. 9, no. 1, pp. 10–26, 2009.

[7] M.C. Smith and F-C.Wang, Performance benefits in passive vehicle suspensions employing inerters, *Veh. Syst. Dyn.* 42(4), pp. 235–257, 2004.

[8] F. Scheibe and M.C. Smith, Analytical solutions for optimal ride comfort and tyre grip for passive vehicle suspensions, *Veh. Syst. Dyn.* 47, 1229–1252, 2009.

[9] S. Evangelou, D.J.N. Limebeer, R.S. Sharp, and M.C. Smith, Steering compensation for high-performance motorcycles, *Proceedings of the 43rd IEEE Conference on Decision and Control*, Paradise Island, pp. 749–754, 2004.

[10] F-C. Wang and C.W. Chen, Performance analysis of building suspension control with inerters, *Proceedings of the 46th IEEE Conference on Decision and Control, New Orleans*, Louisiana, USA, 12-14 December, pp. 3786–3791, 2007.

[11] M.Z.Q. Chen, *Passive network synthesis of restricted complexity*, Ph.D. Thesis, Cambridge Univ. Eng. Dept., U.K., 2007.

[12] M.Z.Q. Chen and M.C. Smith, Electrical and mechanical passive network synthesis, in *Recent Advances in Learning and Control*, New York: Springer-Verlag, vol. 371, 35–50, 2008.

[13] M.Z.Q. Chen and M.C. Smith, A note on tests for positive-real functions, *IEEE Trans. on Automatic Control*, vol. 54, no. 2, 390–393, 2009.

[14] M.Z.Q. Chen and M.C. Smith, Restricted complexity network realizations for passive mechanical control, *IEEE Trans. on Automatic Control*, vol. 54, no. 10, 2290–2301, 2009.

[15] A. Hać and H. Youn, Optimal semi-active suspension with preview based on a quarter car model, *Proceedings of the American Control Conference*, Boston Massachusetts, June 1991.

[16] S.M. Savaresi, C. Poussot-Vassal, C. Spelta, O. Sename, and L. Dugard, *Semi-Active Suspension Control Design for Vehicles*. Elsevier, Butterworth Heinemann, 2010.

[17] D. Hrovat, Survey of advanced suspension developments and related optimal control applications, *Automatica*, 33:1781–1817, 1997.

[18] C. Poussot-Vassal, S.M. Savaresi, C. Spelta, O. Sename, and L. Dugard, A methodology for optimal semi-active suspension systems performance evaluation, *In: Proc. 49th IEEE Conf. Dec. Contr.*, Atlanta, GA, pp. 2892–2897, 2010.

[19] N. Giorgetti, A. Bemporad, H.E. Tseng, and D. Hrovat, Hybrid model predictive control application towards optimal semi-active suspension, *International Journal of Control*, vol. 79, no. 5, pp. 521–533, 2006.

[20] A.E. Bryson and Y.C. Ho, *Applied Optimal Control*. Waltham, MA: Blaisdell, 1969.

[21] S.M. Savaresi and C. Spelta, A single-sensor control strategy for semi-active suspensions, *IEEE Transaction on Control System Technology*, vol. 17, no. 1, pp. 143–152, January 2009.

[22] A. Hać, Optimal linear previewcontrol of active vehicle suspension, *Veh. Syst. Dyn.*, vol. 21, pp. 167–195, 1992.